Chapter 2
Negative Refraction and Acoustical Cloaking

Abstract Negative refraction is not only the consequence of the negative mass density and negative bulk modulus of the acoustical metamaterial but also can produce phononic crystal's band gap. Acoustical cloaking is an application of the form invariance of the acoustic field equation. It is the first application of sound propagation in curvilinear space-time. It enables the bending and the manipulation of the direction of the sound wave to our requirement. Both negative refraction and acoustical cloaking can be derived from coordinates transformation of the acoustic field equation. In fact, negative refraction is a special case of acoustical cloaking when the value of the determinant of the coordinates transformation equals -1. Negative refraction enables the production of super-resolution lens and acoustical cloaking can be used for shielding objects.

2.1 Introduction

The phenomenon of negative refraction was first theoretically mentioned in Veselago's 1968 [1] paper with idea taken from Mandel'stam's [2] 1945 paper. This is the outcome of the two key parameters of electromagnetic waves: permittivity and permeability having negative values. The material having these properties is known as double negative metamaterial (DNG). It is a special type of metamaterial. This paper did not receive much attention because it was not possible to fabricate double negative metamaterial (DNG) although the other important form of metamaterial, the band gap metamaterial such as photonic crystals and phononic crystals was fabricated much earlier in the 1980s and in the early 1990s, respectively, and photonic crystals were known more than 100 years ago by Lord Rayleigh. In 1999 Pendry et al. [3] of Imperial College London successfully introduced the theoretical concept of split-ring resonator (SRR). This was a great contribution to the field of double negative metamaterial (DNG) as his theoretical concept enabled Smith [4] of Duke University USA to successfully fabricate experimentally the double negative metamaterial (DNG) using the concept of SRR. Then, there was great increase in interests in double negative metamaterials.

W.S. Gan, *New Acoustics Based on Metamaterials*, Engineering Materials,
https://doi.org/10.1007/978-981-10-6376-3_2

Metamaterials are artificial materials engineered to have properties that may not be found in nature. Metamaterials usually gain their properties from structure rather than composition, using small inhomogeneities to create effective macroscopic behaviour. It is a high-level form of composite material with periodic structure. Double negative metamaterials (DNG) also known as left-handed material because the negative directions of the permittivity, the permeability and the Poynting vector will form an anticlockwise rotation.

The phenomenon of negative refraction of left-handed symmetry can be considered and explained in the light of gauge theory. Maxwell's equation is the oldest gauge theory, Left-handed symmetry and the negative values of permeability and permittivity can be regarded as gauge condition. With the substitution of this gauge condition, there is no change in the form of the Maxwell's equations or Maxwell's equation is invariant with respect to a set of negative values of permeability and permittivity. In a subsequent section, acoustical cloaking uses the concept of gauge invariance of the Maxwell's equation subjected to curvilinear coordinate transformations (used in general relativity) and metamaterial. This reconfirms that negative refraction and acoustical cloaking can be explained in terms of gauge invariance.

2.2 Limitation of Veselago's Theory

2.2.1 Introduction

Veselago [1] proposed in 1968 the concept of metamaterials for electromagnetic waves having simultaneous negative values of the permittivity and the permeability, or double negativity. In this section, we point out the limitation of Veselago's [1] theory. Veselago's [1] theory is based on the dispersion relation for isotropic solids. Our new approach or alternative approach is based on the gauge invariance approach to acoustic fields proposed by the author in 2007 [5]. We show that this approach can extend metamaterials from electromagnetic waves to acoustic waves from first principles without using analogy. Also it can remove the ambiguity of using the dispersion relation for the refractive index because both the positive and the negative signs for the refractive index simultaneously occur due to the square root sign and this has to be justified. In addition, it is applicable to acoustical cloaking using coordinates transformation, a form of gauge invariance. We also discover parity invariance in acoustic field equations although the Maxwell's equations are known to be parity invariant. Electromagnetic metamaterials are materials with artificial electromagnetic properties defined by their sub-wavelength structure rather than their chemical composition. The left-handed metamaterials are a special type of metamaterial with parity p equals -1 and having the properties of negative permittivity and negative permeability and with the Poynting vector for energy flow in the opposite direction to that of wave propagation.

2.2.2 Gauge Invariance of Homogeneous Electromagnetic Wave Equation

Veselago [1] started with the dispersion relation for the propagation of electromagnetic wave in isotropic material. He considered the dispersion relation

$$k^2 = \frac{\omega^2}{c^2} n^2 \tag{2.1}$$

and

$$n^2 = \varepsilon\mu \tag{2.2}$$

where k = wave number, ω = frequency, c = wave velocity, n = index of refraction of the medium, ε = permittivity and μ = permeability.

Neglecting losses and regarding n, ε and μ as real numbers, it can be seen from (2.1) and (2.2) that a simultaneous change of the signs of ε and μ has no effect on these relations. That is, (2.1) and (2.2) are also valid for $-\mu$ and $-\varepsilon$. He then shows that for $\varepsilon > 0$ and $\mu > 0$ then $\vec{E}, \vec{H}$ and k form a right-handed triplet of vectors and if $\varepsilon < 0$ and $\mu < 0$ they form a left-handed set where $\vec{E}$ = electric field and $\vec{H}$ = magnetic field. He then introduced direction cosines for the vectors $\vec{E}, \vec{H}$ and $\overrightarrow{k}$ and denote them by α_i, β_i, and γ_i respectively, to characterize wave propagation in a medium:

$$G = \begin{pmatrix} \alpha_1 & \alpha_2 & \alpha_3 \\ \beta_1 & \beta_2 & \beta_3 \\ \gamma_1 & \gamma_2 & \gamma_3 \end{pmatrix} \tag{2.3}$$

The determinant of this matrix is equal to +1 if the vectors $\vec{E}, \vec{H}$ and $\overrightarrow{k}$ are a right-handed set and −1 if this set is left-handed. He then denoted this determinant by p and said that p characterized the "rightness" of the given medium. That is, the medium is "right-handed" if $p = +1$ and "left-handed" if $p = -1$.

In this section, I replace "rightness" by parity and parity = −1 is for left-handed set and parity = +1 is for right-handed set. Parity is the language of gauge invariance. All physics laws obey parity invariance except the *β decay in weak interaction*.

Also Poynting vector $\vec{S}$ which denotes energy flow and the parameter of highest interest in electromagnetic wave is given by

$$\vec{S} = \frac{c}{4\pi} \left[\vec{E} \wedge \vec{H}\right] \tag{2.4}$$

From (2.4), the vector $\vec{S}$ always forms a right-handed set with the vectors $\vec{E}$ and $\vec{H}$. Accordingly, for right-handed substances $\vec{S}$ and k are in the same direction and for left-handed substances, they are in opposite directions [1]. Since the vector k is in the direction of the phase velocity, it is clear that left-handed substances with a so-called negative group velocity, which occurs in particular in anisotropic substances or when there is spatial dispersion. That is for left-handed substance or parity = −1, the Poynting vector is of opposite direction to the phase velocity or the direction of wave propagation. For right-handed substance or parity = +1, the Poynting vector is of same direction as the phase velocity.

In this section, we build left-handed metamaterial on the framework of gauge invariance as it covers the both characteristics of left-handed material: negative permeability and negative permittivity and the Poynting vector pointing in the opposite direction to the phase velocity direction.

Next, we will show that the homogeneous electromagnetic wave equation is gauge invariant to negative permeability and negative permittivity.

For homogeneous medium, the electromagnetic wave equations can be given as:

$$\nabla^2\vec{E} - \frac{\varepsilon\mu}{c^2}\ddot{\vec{E}} = 0, \quad \nabla^2\vec{H} - \frac{\varepsilon\mu}{c^2}\ddot{\vec{H}} = 0 \tag{2.5}$$

We find that there is no change in the form of Eq. (2.5) if ε and μ are to be replaced by $-\varepsilon$ and $-\mu$. This shows the gauge invariance of Eq. (2.5) to negative values of permittivity and permeability.

2.2.3 Gauge Invariance of Acoustic Field Equations

The Helmholtz homogeneous acoustic wave equation is given by

$$\nabla^2 P + \frac{\omega^2}{\rho\kappa}p = 0 \tag{2.6}$$

where p = acoustic pressure, ρ = mass density and κ = bulk modulus.

Again we find that there is no change in the form of Eq. (2.6) if ρ and κ are replaced by $-\rho$ and $-\kappa$. This shows that the Helmholtz wave equation is gauge invariant to the negative values of ρ and κ.

Here, we have extended the left-handed media to acoustics using gauge invariance formulation. We also discover the parity invariance of acoustic field equation instead of using the Veselago's theory. Left-handed media has parity equals −1.

2.2.4 Acoustical Cloaking

Acoustical cloaking is the first introduction of acoustics to curvilinear space-time. Previously, all associations of acoustics with curvilinear space-time are only to describe the geometrical shape of certain structure. They are not dealing with the propagation or bending of sound wave in curvilinear space-time.

Acoustical cloaking deals with the deflection of bending of sound wave and the control of the propagation and direction of sound wave according to our specified direction.

Again Veselago [1]'s theory of using dispersion relation is not relevant here. We use coordinate transformations, a form of gauge invariance. That is, there is no change in the form of the acoustic field equation after the coordinate transformations or the acoustic field equation is gauge invariant subjected to coordinate transformations.

As an illustration, we quoted the results from Cummer [6].

Cummer [6] illustrated coordinate transformations for acoustics by using the linear acoustic equation for inviscid fluid:

$$j\omega p = -\kappa \nabla \cdot \vec{v}, \quad j\omega p\vec{v} = -\nabla p \tag{2.7}$$

where ω = angular frequency, v = sound velocity.

Next, he imposed a new set of curvilinear coordinates x', y′ and z' on these equations. Using A as the Jacobian matrix of coordinate transformations from (x, y, z) to (x', y', z'), he expressed the gradient operation in the new primed coordinates as:

$$\nabla p = A^T \nabla' p = A^T \nabla' p' \tag{2.8}$$

and the divergence operation can be expressed as

$$\nabla \cdot \vec{v} = \det(A) \nabla' \cdot \frac{A}{\det(A)} \vec{v} = \det(A) \nabla' \cdot \overrightarrow{v'} \tag{2.9}$$

With these expressions, the original Eq. (2.7) can be written in the new coordinates as

$$j\omega p' = -\kappa \det(A) \nabla' \cdot \overrightarrow{v'}$$

$$j\omega \det(A) \left(A^T\right)^{-1} \rho \left(A^{-1}\right) \overrightarrow{v'} = -\nabla' p' \tag{2.10}$$

which is in the same form as the original Eq. (2.7) but with the new medium parameters:

$$\kappa' = \det(A)\kappa, \quad \overline{\overline{\rho}} = \det(A) \left(A^T\right)^{-1} \rho \left(A^{-1}\right) \tag{2.11}$$

Physically, this means that if one applies a coordinate transformations to a solution to Eq. (2.7) and changes the medium properties according to Eq. (2.11), the transformed fields are a solution to the acoustic equations in the new medium.

2.2.5 *Gauge Invariance of Nonlinear Homogeneous Acoustic Wave Equation*

The nonlinear homogeneous acoustic wave equation up to the second order can be given as:

$$\kappa_1 \nabla^2 p + \kappa_2 \nabla^2 p \left(\frac{\partial p}{\partial x}\right) + \frac{\omega^2 p}{\rho} = 0$$

or

$$\rho\kappa_1 \nabla^2 p + \rho\kappa_2 \nabla^2 p \left(\frac{\partial p}{\partial x}\right) + \omega^2 p = 0 \tag{2.12}$$

where κ_1 = second-order bulk modulus and κ_2 = third-order bulk modulus.

Again if we replace ρ and κ_1, and κ_2 by $-\rho$, $-\kappa_1$ and $-\kappa_2$, there is no change in the form of Eq. (2.12). In another word, the nonlinear acoustic wave equation is gauge invariant to negative values of ρ, κ_1, and κ_2.

2.2.6 *My Important Discovery of Negative Refraction Is a Special Case of Coordinate Transformations or a Unified Theory for Negative Refraction and Cloaking*

Here, we are considering both cloaking and negative refraction under the umbrella theory of coordinate transformations or gauge invariance of the form of equations under coordinates transformation. This is a pattern of nature and is applicable to all equations of physics covering both Maxwell's equations and the acoustic equation of motion. When the determinant of the direction cosines matrix (or transformation matrix) equals −1, one will have negative refraction or parity equals −1. Also when multiplying the original permittivity and the original permeability by the determinant value of −1 will produce negative values of the permittivity and the permeability. This shows that negative refraction is a special case of coordinate transformations used in cloaking problem when the determinant of the transformation matrix equals −1. This can be illustrated as follows:

$$\begin{pmatrix} v_x' \\ v_y' \\ v_z' \end{pmatrix} = \begin{pmatrix} \propto_1 & \propto_2 & \propto_3 \\ \beta_1 & \beta_2 & \beta_3 \\ \gamma_1 & \gamma_2 & \gamma_3 \end{pmatrix} \begin{pmatrix} v_x \\ v_y \\ v_z \end{pmatrix} \tag{2.13}$$

When the determinant of the direction cosines matrix on the right-hand side of (2.13) equals −1, we have

$$\overrightarrow{v'} = -\vec{v} \tag{2.14}$$

Replacing the vectors by the examples of permeability and permittivity, we will have

$$\overrightarrow{\mu_{ij}'} = -\overrightarrow{\mu_{ij}} \quad \text{and} \quad \overrightarrow{\varepsilon_{il}'} = -\overrightarrow{\varepsilon_{il}} \tag{2.15}$$

This shows that negative refraction also produces negative permeability and negative permittivity.

Since this gauge invariance of the form of equation is a pattern of nature of all physics equations, it is also applicable to the acoustic case where the equivalence of the permittivity and permeability is the mass density and the bulk modulus or compressibility.

This also shows that cloaking material or component will become the lens in the special case of negative refraction, and refraction is a special case of cloaking or the bending of light wave or sound wave when the path of wave propagation becomes linear from nonlinearity.

This shows that gauge invariance has a broader coverage and applications than Veselago [1]'s dispersion relation.

Also reflection invariance (or right-left symmetry) can be introduced to explain negative refraction. In fact, $-\mu$ and $-\varepsilon$ can be considered as the mirror image of μ and ε and $-\rho$ and $-\kappa$ can be considered as the mirror image of ρ and κ. Again here the concept of coordinate transformations is used.

Of course, it should be also mentioned here that gauge invariance approach to negative refraction removes the ambiguity caused by using the dispersion relation. There are both positive and negative signs occur simultaneously due to the square root sign of the dispersion relation and this has to be justified.

2.2.7 *Conclusions*

The above evidence shows that Veselago's [1] theory is applicable only to electromagnetic waves and for isotropic materials and for the special case of double negativity and for linear case. Gauge invariance approach on the other hand has broader applications even to acoustic waves, to anisotropic materials, to cloaking problems, to negative refraction and to nonlinear acoustics. It also has the important

contribution of removing the ambiguity occurred of whether to use the positive or the negative sign of the dispersion relation.

In fact after Smith's [4] and Pendry's [3] accomplishments with metamaterials, Veselago realized that the most important contribution of his original 1968 paper is not that a composite material can be designed to produce a negative refraction, but that a composite material can be designed to produce any value for permittivity and permeability. This reconfirms my important discovery that negative refraction or double negativity in permittivity and permeability is only a special case of the general case of cloaking using coordinate transformations where a composite material can be designed to produce any value for permittivity and permeability.

2.3 Multiple Scattering Approach to Perfect Acoustic Lens

The multiple scattering theory (MST) usually known as the KKR (Korringa, Kohn and Rostoker) approach [7, 8] was developed mainly for the calculation of electronic band structures although it originated from the study of classical waves including acoustic waves used by Liu et al. [9] to calculate the propagation of sound waves in periodic structures such as phononic crystals. The phononic crystals in this case are stainless steel balls immersed in water. They found theoretically and experimental agreement using ultrasound experiment of the observation of a sizable directional stopband in the transmission along (001) centred at about 0.65 units, coincides with unexpectedly directional gap along the $\Gamma - x$ direction in the band structure. In the transmission along (111) they observed a narrow stopband at about 0.65 units, corresponding to the small gap at the L point in the band structure at the same frequency.

Other works on the studies on the existence and properties of phonon band gap are [10–13]. These are due to Bragg scattering when the sound wavelength is comparable with the lattice constants. This leads to frequency bands where wave propagation is forbidden. This enables the understanding of how to achieve large complete band gaps in physically realizable materials and the mechanism of wave transport at band frequencies due to tunnelling [14]. Also there has been relatively less attention paid to investigate how periodicity affects wave propagations over a wide range of frequencies outside the band gaps where novel refraction, diffraction and focusing effects may be possible.

At low sound frequencies, an effective continuum or medium approximation can be used to study the wave properties and accurately predict the wave speed. In this frequency range, there is much in common with the properties of low-frequency phonons in atomic crystals, where phonon focusing phenomena have been systematically studied [15]. However, at higher frequencies, much less is known about the behaviour in pass bands where the wavelengths can be much less than the lattice constant. Suxia Yang et al. [14] have addressed this problem by theoretically and experimentally investigating the character of wave pattern and propagation in a 3D phonon crystal at frequency above the first complete band gap. They showed how a

dramatic variations in wave propagation with both frequency and propagation direction can lead to novel focusing phenomena associated with large negative refraction. This is a different approach to negative refraction from that of Veselago's work for the electromagnetic wave based on negative values of permittivity and permeability. They demonstrated the effect of negative refraction experimentally by using ultrasound technique to image the transmitted wave field and show that a flat crystal can focus a diverging incident beam into a sharp focal spot that can be seen remarkably far from the crystal.

They also calculated the field pattern theoretically using a Fourier imaging technique in which wave propagation through the crystal is accurately described by the 3D equifrequency surfaces predicted from the multiple scattering theory (MST) [16]. Their theoretical results also give an excellent explanation of the experimental data, showing how wave physics in the regime can be accurately modelled and how the theoretical structures on the equifrequency surfaces of phonon crystal can give rise to potential applications.

Zhang and Liu [17] first discussed the issue of negative refraction for acoustic waves in phononic crystals. They also repeated the observation of the negative refraction of acoustic wave in phononic crystals, occurring at the frequencies with $\vec{S} \cdot \vec{k} > 0$ where $\vec{S}$ represents the Poynting vector. They considered a 2D phononic crystal consisting of infinite-length "rigid" or liquid cylinders embedded in a background which have been studied extensively in Refs. [18–20]. Two types of phononic crystals were used by them. One is steel cylinders in air background, and the other is water cylinders in mercury background. The band structures of these two types of phononic crystals were plotted in Fig. 2.1a, b, respectively. Both of them were calculated by the MST (or Korringa-Kohn-Rostoker method given in Ref. [21]).

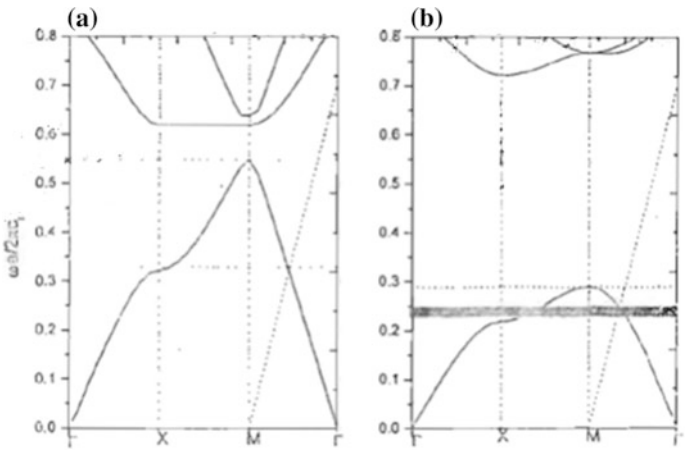

Fig. 2.1 **a** The acoustic band structures for a square lattice of steel cylinders in air background, with cylinder radius $R = 0.36a$. **b** The acoustic band structures for a square lattice of water cylinders in mercury background with cylinder radius $R = 0.4a$. The light line shifted to M is shown in dashed line. Dot-dashed lines mark the region for negative refraction and the shadow represent the AANR region. From Zhang and Liu [17]

To visualize and analyse refractive effects of the acoustic wave when it hits the above phononic crystal interfaces, Zhang et al. [17] investigated the equifrequency surfaces (EFS) of the band structures just like the case for the electromagnetic waves in the photonic crystals because the gradient vector of constant-frequency contours ink-space give the group velocities of the phononic modes. Hence, the propagation direction of energy velocity of acoustic wave can be reduced from them. The EFS can also be calculated using the MST or the Korringa-Kohn-Rostoker method. The features of the EFS for these two kinds of system within the first band are similar. Thus, only the results of water-mercury system with $R = 0.4a$ in given in Fig. 2.2. The equifrequency surface contours at several relevant frequencies such as 0.05, 0.1, 0.2, 0.235 and 0.27 are demonstrated. It is clear that the lowest band has $\vec{S} \cdot \vec{k} > 0$ everywhere within the first Brillouin zone, meaning that the group velocity is never opposite to the phase velocity. The 0.05 and 0.1 contours are very close to a perfect circle, and the group velocity at any point of the contour is collimated with the k vector, indicating that the crystal behaves like an effective homogeneous medium at these two long wavelengths.

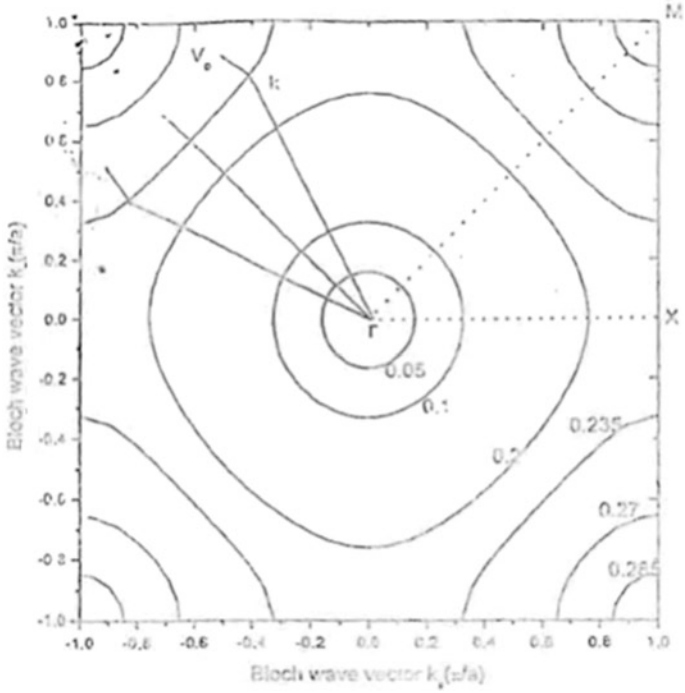

Fig. 2.2 Several constant-frequency contours of the first band of the 2D phononic crystal, which is composed of a square lattice of water cylinders in mercury background with $R = 0.4a$. The numbers in the figure mark the frequencies in unit of $2\pi c_l/a$

The 0.2 contour is a little bit distorted from a circle, and the 0.235 contour is convex around the M point due to a negative phononic "effective band". The conservations of the component along the surface of refraction would result in the negative refractions effect in some frequency region, marked as dotted lines in Fig. 2.1.

Furthermore, according to the analysis approach of [18, 22], the required condition for all-angle negative refraction (AANR) effect in some cases can be observed. Under these conditions, an acoustic beam incident on the ΓM surface with various incident angles will couple to a single Bloch mode that propagates into this crystal on the negative side of the boundary normal. Therefore, we can define a frequency region for the AANR by using these criteria.

From Fig. 2.1a, we noted that the AANR region is absent in the steel-air system, although the negative refractive region is very large. However, in the water-mercury system, the AANR region exists within the range of about 63 near $\omega = 0.24(2\pi c_l/a)$ (shadow region in Fig. 2.1b). This point differs from the two kinds of system. This difference is very important for the superlensing and focusing of acoustic waves in phononic crystals.

In order to test this theoretical analysis, Zhang et al. [17] performed a numerical simulation to the two phononic crystals system based on the MST [19]. They used a 30° wedged sample which consisted of 238 water cylinders of $R = 0.4a$ in the mercury background with a square array. The shape of the sample and an illustration of the refraction process are shown on the top of Fig. 2.3. The black frame marked the boundaries and the size of the sample. The wedged surface was the (11) surface when a slit beam of frequency $\omega = 0.235(2\pi c_l/a)$ with a half-width $wl = 2a$ incident normal to the left surface of the sample, it transports along the direction of incidence wave until it meets the wedge (11) interface of the sample, and then a part of it will refract outside of the sample and the other reflect inside. There are two possibilities for the refracted wave. It may travel on the right side (positive refraction) or left side (negative refraction) of the surface normal. The simulation results are plotted in Fig. 2.3. The field energy pattern of the incidence and refraction is shown in the figure. The arrows and text illustrate the various beam directions. It can be clearly seen that the density flux of the refractive wave outside of the sample travels on the negative refraction side of the surface normal. The refraction angle is consistent with the estimation from the wave vector space in Fig. 2.2. The simulation results show clearly that the negative refraction of the acoustic wave exists in the first band for the case with $\vec{S} \cdot \vec{k} > 0$. Similar phenomena have also been demonstrated in the steel-air system.

The concept of perfect lens or microsuperlens has been designed using the concept of negative refraction [1, 20] and fabricated with 2D photonic crystals [18].

Such a superlens can focus a point source on one side of the lens into a real point image on the other side even for the case of a parallel sided slab of material. The advantage of the superlens or perfect lens is the capability to defeat the diffraction limit or Rayleigh resolution criterion of wavelength divided by two. Such an image

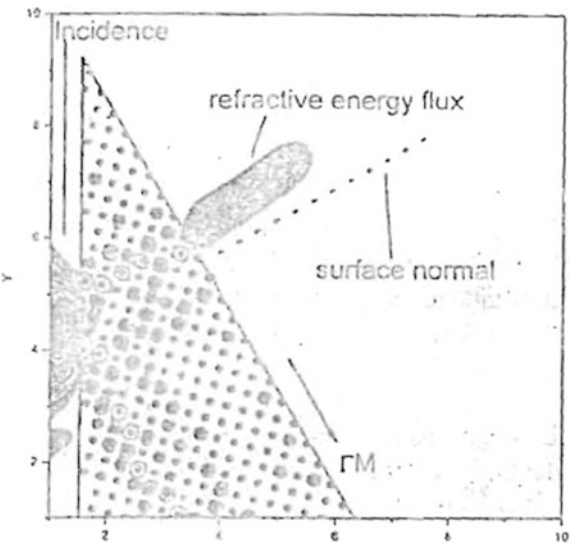

Fig. 2.3 Simulation of negative refraction. The boundaries of the sample are marked with black frame. The intensity of pressure field for incidence and refraction are shown in different shadows. A wedged sample considered here consists of water cylinders in mercury background with $R = 0.4a$ as shown on top of the figure. The frequency of incident wave is $\omega = 0.235(2\pi c_l/a)$

can be realized by flat slab instead of curved shapes and thus fabrications can be easier in principle. Zhang and Liu [17] demonstrated the design of such a perfect lens for sound waves which possess the same advantage as that of optical system. They used a slab of the sample with $40a$ width and six layers thick. A continuous wave point source is placed at a distance $1.0a$ from the left surface of the slab. The frequency of the incident wave emitting from such a point source is $\omega = 0.24(2\pi c_l/a)$, chosen to be within the region where all-angle negative refractions may occur (Fig. 2.1b).

The MST method is used to calculate the propagation of an acoustic wave in such a system. The typical results of field pattern of pressure wave and their images across the slab sample are given in Fig. 2.4. The geometry of the phononic crystal slab is also displayed. One can find quite a high-quality image formed in the opposite side of the slab. A closer look at the data reveals a transverse size (full size at half-maximum) of the image spot as $0.6a$ (or 0.14λ) at a distance of $1.0a$ from the right surface of the slab. The focusing size of the image depends on certain parameters such as the thickness of the slab and the distance between the source and the slab which is similar to the case for the optical system. The tuning of these parameters will produce a clearer acoustic image.

They also studied the effect on the image quality when the frequency of the sound wave is outside of the AANR region and system without the AANR region such as steel-air system. For these cases, the focusing phenomena are degraded. These show that the AANR is very important for the image formations.

This shows that negative refraction for acoustic wave in the 2D phonons crystal exists in a manner similar to that of optics.

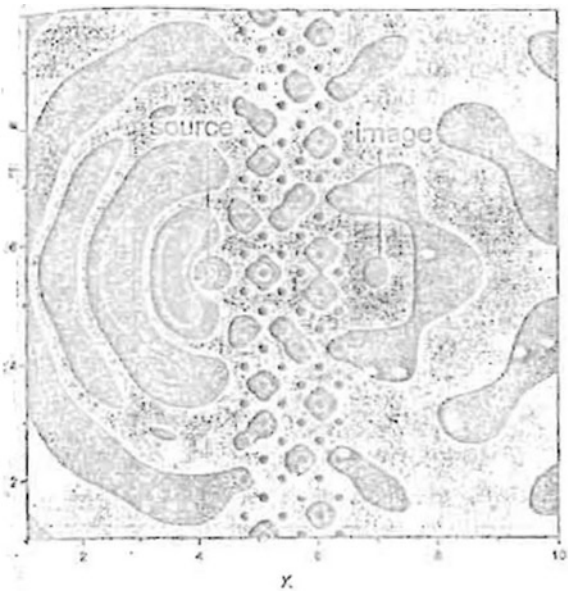

Fig. 2.4 Field pattern of pressure wave of a point source and its image across a six-layer slab at frequency $\omega = 0.24(2\pi c_l/a)$. The system considered here consists of some water cylinders in mercury background with $R = 0.4a$. Dark and bright regions correspond to negative and positive values, respectively

2.4 Acoustical Cloaking

2.4.1 Introduction

Acoustical cloaking can be classified as a form of acoustical imaging because by placing a metamaterial acoustical cloak on the object to be cloaked it will render its disappearance from one sight. The concept of acoustical cloaking also extended from electromagnetic cloaking [21, 23]. Electromagnetic cloaking uses concepts of gauge invariance from general relativity that is the form of the Maxwell's equations remain unchanged under arbitrary coordinate transformations with transformed permittivity and permeability values which are scaled by a common factor. Because of the nature of negative refraction of metamaterial, by cloaking the object with a metamaterial, the light rays will be deflected, stretched and bended and guided around the object and returned to their original trajectory.

However, due to the dispersion nature of the light, the cloaking effect is specific only to a single frequency and not broadband.

The concept of acoustical cloaking was extended to acoustics by Milton et al. in 2006 [24] and by Cummer and Schurig in 2007 [6]. The analysis by Milton et al. [24] indicated that the coordinate transformations approach cannot be extended to elastodynamic waves in solids in the fully general case or even for the special case of compressional waves in a fluid. However, a scattering theory analysis has shown that the cloaking solution exists for acoustic waves in fluids as three dimensions [25–27] and by analogies with electromagnetics. It has been shown that 2D acoustic waves [6] and 3D acoustic waves [28] can be made transformation invariant.

The material parameters required to implement acoustic coordinate changes have also been obtained by Greenleaf et al. [29].

It has to be noted that the phenomenon of acoustical cloaking cannot be transplanted blindly from electromagnetic cloaking using analogy. As shown in Sect. 2.2, Veselago's [1] theory is not applicable to acoustic waves and even for electromagnetic waves is valid only to isotropic case and not for anisotropic cloaking material which most cloaking materials are made of. Also the acoustic metamaterial has to be derived using the theory of elasticity and not from dispersion relation as what used to derive the Veselago [1]'s negative permeability and negative permittivity. Our gauge invariance approach can provide better physical understanding of negative refraction and cloaking. We also noted that acoustic negative refraction can be obtained from multiple scattering theory (MST) besides the approach of negative mass density and negative bulk modulus. This also confirms negative refraction is a form of multiple scattering. The above analysis is also given in Sect. 2.2.

Our idea of objection to use analogy between acoustic wave and electromagnetic wave is supported by Cummer et al. [25]. They pointed out that demonstrating the invariance through analogy of acoustic wave with electromagnetic wave masks some of the physics of the transformations approach particularly how vectors such as particle velocity and the pressure gradient change under transformation. Through an analysis of how power flow and constant phase surfaces must transform for completely general waves, they show that the velocity vector in acoustics must transform in a different way than the $\vec{E}$ and $\vec{H}$ *vectors* in electromagnetics. This explains why Milton et al.'s [24] elastodynamics analysis which assumed that the acoustic velocity transforms like $\overrightarrow{E}$ and $\overrightarrow{H}$ did not result in acoustic equation transformation invariance. We feel that this further shows the intrinsic elastic properties of acoustic wave as different from the electromagnetics. The treatment of negative refraction using theory of elasticity approach by Lee et al. [30] and Gan's analysis on the gauge invariance of acoustic fields [5] further confirm this. An example of the fabricating of acoustical cloak is given by Cheng et al. [31].

2.4.2 *Derivation of Transformation Acoustics*

Here, we follow approach of Cummer et al. [26]. The fluids version of the linear acoustic field equations will be used:

$$\nabla p = i\omega\rho(\vec{r})\rho_0\vec{v} \tag{2.16}$$

$$i\omega p = \kappa(\vec{r})\kappa_0\nabla\cdot\vec{v} \tag{2.17}$$

where $\rho(\vec{r})$ and $\kappa(\vec{r})$ are the normalized density and bulk modulus, respectively, of the medium and are coordinate transform invariant. We will demonstrate how the

acoustic velocity vector $\vec{v}$ must transform by considering $\vec{v}$ in a nonorthogonal coordinate system described by coordinate q_1, q_2 and q_3 with unit vectors $\hat{u}_1$,$\hat{u}_2$ and $\hat{u}_3$, respectively. Following Pendry et al. [23] and letting $i = 1, 2, 3$

$$Q_i^2 = \left(\frac{\partial x}{\partial q_i}\right)^2 + \left(\frac{\partial y}{\partial q_i}\right)^2 + \left(\frac{\partial z}{\partial q_i}\right)^2 \tag{2.18}$$

$$\hat{n} = (\widehat{u_1} \times \widehat{u_2})/(/\widehat{u_1} \times \widehat{u_2}/)$$

$$\text{Area} = Q_1 \mathrm{d}q_1 Q_2 \mathrm{d}q_2 |\hat{u}_1 \times \hat{u}_2|$$

Figure 2.5 shows what happens when we apply the divergence theorem to an infinitesimal volume in this nonorthogonal coordinate system.

Deriving the net outward flux of $\vec{v}$ from this volume and setting it equal to the divergence of $\vec{v}$ times the infinitesimal volume, it can be shown that

$$(\nabla \cdot \vec{v}) Q_1 Q_2 Q_3 |\hat{u}_1 \cdot (\hat{u}_2 \times \hat{u}_3)| = \frac{\partial}{\partial q_1}[Q_2 Q_3 \vec{v} \cdot (\hat{u}_2 \times \hat{u}_3)] + \frac{\partial}{\partial q_2}[Q_1 Q_3 \vec{v} \cdot (\hat{u}_1 \times \hat{u}_3)] + \frac{\partial}{\partial q_3}[Q_1 Q_2 \vec{v} \cdot (\hat{u}_1 \times \hat{u}_2)] \tag{2.19}$$

Let $V_{\text{frac}} = |\hat{u}_1 \cdot (\hat{u}_2 \times \hat{u}_3)|$ because this is the fraction by which a unit volume is compressed by the coordinate nonorthogonality and we use the conventional superscript (subscript) notation for contravariant (covariant) vector components using

$$\vec{v} \cdot (\hat{u}_2 \times \hat{u}_3) = v^1 \hat{u}_1 \times (\hat{u}_2 \times \hat{u}_3) \tag{2.20}$$

Equation (2.19) can be rewritten as

$$(\nabla \times \vec{v}) Q_1 Q_2 Q_3 V_{\text{frac}} = \frac{\partial}{\partial q_1}\left(Q_2 Q_3 V_{\text{frac}} v^1\right) + \frac{\partial}{\partial q_2}\left(Q_1 Q_3 V_{\text{frac}} v^2\right) + \frac{\partial}{\partial q_3}\left(Q_1 Q_2 V_{\text{frac}} v^3\right) \tag{2.21}$$

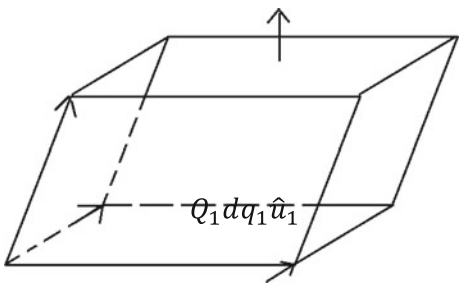

Fig. 2.5 Parallel piped that defines an infinitesimal volume in the transformed coordinates. The area and unit normal of each face enter in the calculation of the net flux of a vector out of this volume. From Cummer et al. [26]

Noting that the divergence in the transformed coordinates is defined by $\nabla_q \cdot \vec{v} = \frac{\partial v^1}{\partial q_1} + \frac{\partial v^2}{\partial q_2} + \frac{\partial v^3}{\partial q_3}$, we can write

$$(\nabla \cdot \vec{v}) Q_1 Q_2 Q_3 V_{\text{frac}} = \nabla_q \cdot (V_{\text{frac}} \overline{\overline{Q}}_{\text{per}} \left[v^1 v^2 v^3\right]^T = \nabla_q \cdot \tilde{v} \tag{2.22}$$

where

$$\overline{\overline{Q}}_{\text{per}} = \begin{bmatrix} Q_2 Q_3 & 0 & 0 \\ 0 & Q_1 Q_3 & 0 \\ 0 & 0 & Q_1 Q_2 \end{bmatrix} \tag{2.23}$$

and the transformed velocity vector $\tilde{v}$ is given by

$$\tilde{v} = V_{\text{frac}} \overline{\overline{Q}}_{\text{per}} \left[v^1 v^2 v^3\right]^T \tag{2.24}$$

The per subscript on the tensor $\overline{\overline{Q}}_{\text{per}}$ is to denote that the diagonal elements transform each vector component by the product of the coordinate scaling factors perpendicular (more general, not parallel, for the case of nonorthogonal coordinates) to the direction of the vector component. Recall that our qualitative discussion above, summarized in Fig. 2.6, showed that this is precisely how the velocity vector must transform in a compressed wave in order for transformation acoustics to work. Note that the elements of the volume vector $\left[v^1 v^2 v^3\right]^T$ are the contravariant components of $\vec{v}$ in the nonorthogonal coordinate system while the element of the vector $\vec{v}$ is the component in the original orthogonal coordinate system.

Multiplying (2.17) (with $\lambda(\vec{r}) = 1$) by $Q_1 Q_2 Q_3 V_{\text{frac}}$ and using (2.24) results in the equation in the transformed coordinates,

$$i\omega p = \kappa(\vec{q}) \kappa \nabla_q \cdot \tilde{\vec{v}} \tag{2.25}$$

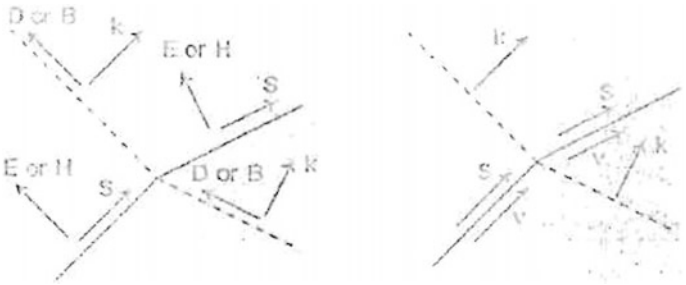

Fig. 2.6 Transformation of vectors in electromagnetic (left) and acoustic or compressional elastodynamic (right). The white converging arrows denote which component of each vector is compressed by the coordinate transformations. From Cummer et al. [26]

with

$$\kappa(\overline{q}) = (Q_1 Q_2 Q_3 V_{\text{frac}})^{-1} \tag{2.26}$$

This demonstrates the coordinate to function invariant of (2.17) provided that the bulk modulus is modified according to (2.26) and the velocity vector is transformed according to (2.25). More generally, this also shows how a vector must transform in order for the gradient operator to maintain its basis form.

Cummer et al. [26] derived how (2.16) and therefore the gradient operator transforms under a coordinate change using the gradient theorem and integrating ∇p along a short length in the q_1 coordinate directions, they find that

$$\nabla p \cdot Q_1 \hat{u}_1 = \frac{\partial p}{\partial q_1} = \left(\nabla_q p\right)^1 \tag{2.27}$$

The left-hand side contains the scaled covariant components of ∇p which must be converted to covariant components before it can be equated component-wise to $\nabla_q p$, the gradient in the transformed coordinates. They find that

$$\nabla_q p = \overline{\overline{Q}}_{\text{par}} \overline{\overline{h}}^{-1} (\nabla p) \tag{2.28}$$

where $\overline{\overline{Q}}_{\text{par}}$ is the diagonal tensor containing coordinate scaling factors parallel to the direction of the vector component or

$$\overline{\overline{Q}}_{\text{par}} = \begin{bmatrix} Q_1 & 0 & 0 \\ 0 & Q_2 & 0 \\ 0 & 0 & Q_3 \end{bmatrix} \tag{2.29}$$

and

$$\overline{\overline{h}}^{-1} = \begin{bmatrix} \hat{u}_1 \cdot \hat{u}_1 & \hat{u}_1 \cdot \hat{u}_2 & \hat{u}_1 \cdot \hat{u}_3 \\ \hat{u}_2 \cdot \hat{u}_1 & \hat{u}_2 \cdot \hat{u}_2 & \hat{u}_2 \cdot \hat{u}_3 \\ \hat{u}_3 \cdot \hat{u}_1 & \hat{u}_3 \cdot \hat{u}_2 & \hat{u}_3 \cdot \hat{u}_3 \end{bmatrix} \tag{2.30}$$

Note that this $\overline{\overline{h}}^{-1}$ is the same as $\overline{\overline{g}}^{-1}$ defined by Pendry et al. [23]. They rename this tensor because they will use $\overline{\overline{g}}$ later to denote the metric tensor which is not quite the same as this $\overline{\overline{h}}$.

Finally multiplying (1) (with $\rho(\vec{r}) = 1$) by $\overline{\overline{Q}}_{\text{par}}$, they find

$$p_q p = i\omega \overline{\overline{Q}}_{\text{par}} \overline{\overline{h}}^{-1} \rho_0 \vec{v} = i\omega \overline{\overline{Q}}_{\text{par}} \overline{\overline{h}}^{-1} \overline{\overline{Q}}_{\text{par}}^{-1} V_{\text{frac}}^{-1} \rho_0 \vec{v} \tag{2.31}$$

leaving us with the equivalent of (12.16) in fully transformed coordinates:

$$\nabla_q p = i\omega\overline{\overline{\rho}}\rho_0\vec{v} \tag{2.32}$$

with

$$\overline{\overline{p}} = \overline{\overline{Q}}_{\text{par}}\overline{\overline{h}}^{-1}\overline{\overline{Q}}_{\text{par}}^{-1}\overline{\overline{V}}_{\text{frac}}^{-1} \tag{2.33}$$

Equations (2.25) and (2.32) show that the acoustic equations are fully transformation invariant with the modified material parameters in (2.26) and (2.33).

They further show that these experiments are equivalent to those shown by Chen and Chan [24] purely by analogy with electromagnetics through the electric conductivity equation [32] and those derived by Greenleaf et al. [29] for the general scale Helmholtz equation. Consequently, cloaking shell, concentrator and other devices that have been designed theoretically by electromagnetics can also be realized for acoustics provided that the bulk modulus and anisotropic effective mass density tensor can be realized in practice as specified by (2.26) and (2.33). This first principles derivation without using analogy shows explicitly in (2.24) how the acoustic velocity vector must transform under coordinate change, which as noted above is different from how the $\vec{E}$ and $\vec{H}$ field, transform in electromagnetics. The scalar pressure is, however, not changed by the coordinate transformations and thus like phase fronts and power flow lines is simply deformed by any coordinate transformations.

2.4.3 Application to a Specific Example

We consider the spherical cloaking transformation [6] as illustrated in Fig. 2.7 and specified by $r' = a + r(b-a)/b$ where a and b are constants and $b > a$. This coordinate transformations is orthogonal and then $\overline{\overline{h}} = 1$ and $V_{\text{frac}} = 1$ which are good simplification. The Q_i length scaling factors are straightforward to calculate provided one realizes that the azimuthal and polar angles and not length, as in Cartesian coordinates and (2.18) must be modified slightly. The Q_i is defined by the ratio of infinitesimal lengths in the transformed and untransformed coordinates and thus,

$$Q_r = \frac{\mathrm{d}r}{\mathrm{d}r'} = \frac{b}{b-a}, \quad Q_\phi = \frac{r\mathrm{d}\phi}{r'\mathrm{d}\phi'} = \frac{b}{b-a}\frac{r'-a}{r'} \tag{2.34}$$

$$Q_\Theta = \frac{r\,\sin\,\theta}{r'\,\sin\,\theta'}\frac{\mathrm{d}\theta}{\mathrm{d}\theta'} = \theta_\varphi \tag{2.35}$$

in agreement with the parameter found through other approaches by Chen and Chan [28], Greenleaf et al. [29] and Cummer et al. [27].

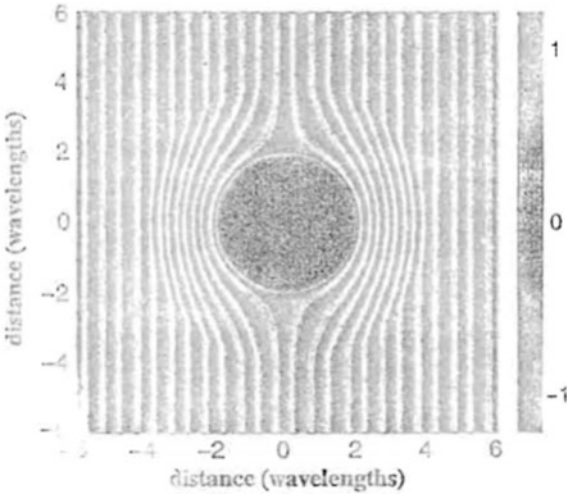

Fig. 2.7 The real part of the pressure field in the $r-\theta$ plane of the problem domain computed from the series solution. The plane wave is incident from the left

Thus, Cummer et al. [26] showed $\vec{E}$ and $\vec{H}$ of electromagnetics transform differently from $\vec{v}$ of acoustic waves under coordinate transformations. It shows that a first principle analysis of the acoustic equation under arbitrary coordinate transformations confirms that the divergence operator is preserved only if velocity transforms in this physically correct way.

2.5 Acoustic Metamaterial with Simultaneous Negative Mass Density and Negative Bulk Modulus

This is a different approach from that of using multiple scattering theory(MST) to produce acoustic negative refraction using phonons crystals [17, 33] (of Sect. 2.3 of MST) and also different from that of the fabrication of acoustical metamaterials for acoustical cloaking based on the invariance of the acoustic field equations under coordinate transformations. The concept is based on the gauge invariance of the acoustic field equations [5]. That is, there is no change in the form of the acoustic field equation with the replacement of the density and bulk modulus by negative density and negative bulk modulus. We have shown in Sect. 2.2 that the concept of negative permittivity and negative permeability giving rise to negative refraction ([1] of Section one) can also be explained by the gauge invariance of the Maxwell's equation with the replacement of the positive permeability and positive permittivity by negative permeability and negative permittivity. In fact, gauge invariance is more appropriate than the approach of Veselago [1] using the dispersive relation as the starting point to introduce negative permeability and negative permittivity as this will give rise to the restriction that only single frequency electromagnetic

cloaking is allowed and also the Veselago [1]'s dispersion relation is used only to the isotropic case whereby most acoustic cloaking materials are anisotropic.

Applying gauge invariance of acoustic fields [34] to negative refraction, broadband double negative spectral range in the structure can be obtained [30]. This is also an experimental verification of my hypothesis on the gauge invariance of acoustic fields [5]. Lee et al. [30] fabricated an acoustic double negativity (DNG) acoustic metamaterial with both membranes and side holes (Fig. 2.8). Here, the acoustic waves are governed by Eqs. (2.36) and (2.37)

$$-\nabla p = \left[\rho - \frac{\kappa}{\omega^2}\right]\frac{\partial \vec{u}}{\partial A} \tag{2.36}$$

and

$$\nabla \cdot \vec{u} = -\left[\frac{1}{B} - \frac{\sigma_{\mathrm{SH}}^2}{\rho_{\mathrm{SH}} A \omega^2}\right]\frac{\partial p}{\partial A} \tag{2.37}$$

where κ = new elastic modulus, $\vec{u}$ = velocity of the fluid (air in this case), ρ = dynamic mass density, B = bulk modulus, A = cross section of the tube, σ_{SH} = SH-cross sectional-density, ρ_{SH} = SH-mass-density.

The existence of the side holes (SH) does not modify Eq. (2.36). Likewise, because the membranes do not sink any fluid, Eq. (2.37) is still valid. Then, the system is described by the dynamic and continuity equations

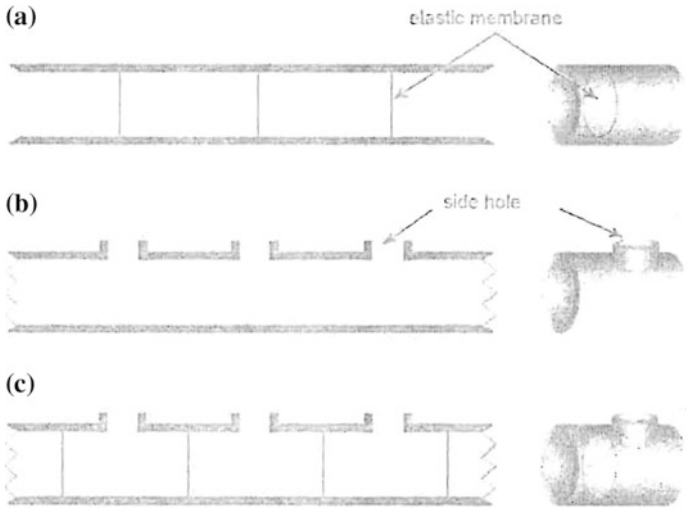

Fig. 2.8 **a** One dimensional SAE structure consisting of thin tensioned elastic membranes in a tube. Negative effective density is observed in this system. **b** A tube with an array of side holes that exhibits negative effective modulus. **c** An acoustic DNG structure with both membranes and side holes. From Lee et al. [30]

$$-\nabla p = \rho_{\text{eff}}\left(\frac{\partial y}{\partial A}\right)\nabla \cdot \vec{u} = -\left(\frac{1}{B_{\text{eff}}}\right)\left(\frac{\partial p}{\partial A}\right)$$

with the effective density and modulus are given by (2.36) and (2.37)

$$P_{\text{eff}} = \rho' - \frac{\kappa}{\omega^2} = \rho'\left[1 - \frac{\omega_{\text{SAE}}^2}{\omega^2}\right] \tag{2.38}$$

$$B_{\text{eff}} = \left[\frac{1}{B} - \frac{\sigma_{\text{SH}}^2}{\rho_{\text{SH}} A\omega^2}\right]^{-1} = B\left[1 - \frac{\omega_{\text{SH}}^2}{\omega^2}\right]^{-1} \tag{2.39}$$

where ω_{SAE} = critical frequency = $\sqrt{\frac{\kappa}{\rho'}}$

The resulting wave equation gives the phase velocity,

$$v_{\text{ph}} = \pm\sqrt{\frac{B_{\text{eff}}}{\rho_{\text{eff}}}} = \pm\sqrt{\frac{B}{\rho'\left(1 - \omega_{\text{SAE}}^2/\omega^2\right)\left(1 - \omega_{\text{SH}}^2/\omega^2\right)}} \tag{2.40}$$

where $\omega_{\text{SH}} = \left(B\sigma_{\text{SH}}^2/A\rho_{\text{SH}}\right)^{1/2}$

The experimental set-up is given in Fig. 2.9a.

It consists of a nonmetal tube on the left and the DNG metamaterial on the right. The absorbers at both ends completely absorb the acoustic energy, preventing any reflection so the system behaves as if it extends to infinity. This eliminates concerns about the effect of the finite number of cells used in the experiment, as well as the interference effect from the reflected waves. The sound source rejects acoustic energy into the tube through a small hole, generating incident waves propagating to the right. At the boundary, a position of the incident energy is reflected and the rest is transmitted into the metamaterial regions. On the metamaterial side, the transmitted acoustic energy flow steadily to the right until it hits the absorber.

Pressure was measured as a function of time and position on both the normal tube side and the metamaterial side. It can be seen that on the normal tube side, the wave proceeds forward, but on the metamaterial side, the wave propagated as indicated by the arrows. Clearly, the wave on the metamaterial propagated in a direction antiparallel to the energy flow. This confirms the theoretical prediction of negative phase velocity. It was noted that the amplitudes and the apparent phase velocity in the normal tube deviated from the actual values of the incident wave because of the interference of the reflected wave from the boundary. In the metamaterial, there is no such interference effect because there is no reflected wave.

The comparison between the theory and experiment is shown in Fig. 2.10.

Theoretically, expected single negative gap is experimentally confirmed by the transmission data (inset). In the DNG and DPS (double positions) pass bands, the phase velocities experimentally determined agree well with the theoretical values. The calculations are given as accurate description of the behaviour of the phase

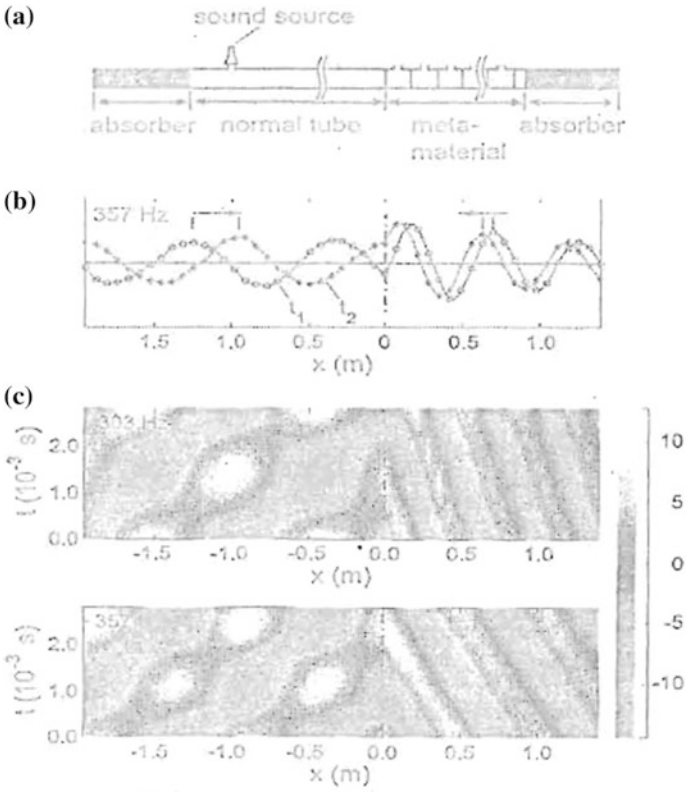

Fig. 2.9 **a** Experimental set-up for the transmission and phase velocity measurements. **b** 'Snapshots' of measured pressure distribution showing backward wave propagation in the metamaterial ($x > 0$). **c** Characteristic diagrams of pressure measurements for the frequencies 303 and 357 Hz. Negative slopes of the wave-paths in the metamaterial sides ($x > 0$) indicate negative phase velocities. From Lee et al. [30]

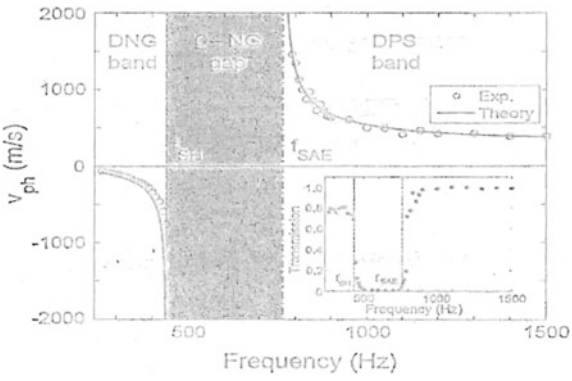

Fig. 2.10 Transmission (inset) and phase velocities of the present acoustic DNG medium. From Lee et al. [30]

velocity in the frequency range from 250 to 1500 Hz. Which is broadband? Because the experiment confirms the theoretical prediction of negative phase velocity, it can be concluded that the density and the bulk modulus actually becomes simultaneously negative in the frequency range below 440 Hz.

We would like to point out the novel concept of spatially anchored elasticity [16] was used. This uses a homogenized structure of membranes to produce negative effective density. This is termed spatially anchored elasticity (SAE) because the fluid is elastically anchored in space by the membranes. The new elasticity can be regarded as an intrinsic variables that characterizing the behaviour of the metamaterial according to Eq. (2.41)

$$\nabla p = -\kappa \vec{\xi} \tag{2.41}$$

where κ = new elastic modulus, ξ = displacement of the fluid, p = pressure of the fluid.

Furthermore, by making additional side holes along the tube wall, acoustic DNG materials were obtained and backward-wave propagation was observed. The constructed structure exhibited DNG characteristic in the spectral range from 240 to 440 Hz which is broadband unlike the electromagnetic case which is limited only to a single frequency due to dispersion. The phase velocity in this band was negative and highly dispersive.

Again this proves that acoustic metamaterial cannot be just transplanted by analogy from the electromagnetic case. It has to be based on the theory of elasticity unlike for the electromagnetic which is based on the dispersion relation of Veselago [1].

2.6 Acoustical Cloaking based on Nonlinear Coordinate Transformations

So far the coordinates transformations used in acoustical cloaking are based on linear coordinate transformations [6]. Akl et al. [35] extended to nonlinear transformation using

$$r^1 = a + (b - a)\left(\frac{r}{b}\right)^n \tag{2.42}$$

where n = an arbitrary transformation exponent that accounts for the degree of nonlinearity in the transformation and can be used as an additional degree of freedom in designing and controlling the bending of the acoustic wave inside the cloak. For unity value of n, the transformation returns back to the linear transformation proposed by Cummer and Schurig [6].

Linear transformation is effective for the case of rigid objects. However, the cloaking becomes less perfect and dependent on the selection domain when flexible

objects are considered where its permeable nature might induce considerable absorption of sound wave which would bring less perfection to the cloak. Akl et al. [35] have presented acoustic cloaking based on different nonlinear coordinate transformations. They developed a finite element model developed through time-harmonic analysis to study the preserve field distribution using different nonlinear coordinate transformations. Such transformations have shown considerable improvements to the cloak performance when applied to flexible objects allowing for wider applicability bandwidth (broadband) as well as for providing additional control of the shape of acoustic wave bending inside the cloak region.

For a metamaterial anisotropic acoustic cloak of a flexible object, the cloak works in a limited frequency range around its resonant frequency. In order to show this fact, a quantifiable measure for the cloak's performance has been developed. They proposed a new performance indicator of the cloak's quality using the acoustic pressure value at a preselected set of points downstream of the cloak. The set of points selected for pressure measurements were distributed along the fluid in such a way to accurately predict the calculation from ideal cloak. The proposed indicator is based on the fact that for ideal cloak, the r.m.s. of the difference between the acoustic pressure values along the wave front downstream of the cloak and a reference value measured along the same wavefront at a reference wave propagation line tend to be zero. A reference wave propagation line located at the middle of the domain is quite a good unbiased choice. This process is repeated with as many planes in the axial direction (along wave propagation lines) and lateral directions as needed to scan the entire fluid domain, where the sum of all the calculated values is divided by the number of measurement points as given in Eq. (2.43)

$$\text{P.I.} = \sum_{j=1}^{j_{\max}} \sqrt{\sum_{i=1}^{i_{\max}} \left(P_{i,j} - P_{i,\text{ref}}\right)^2} \tag{2.43}$$

to yield the targeted performance indicator (P.I.). The measurement grid points are as illustrated in Fig. 2.11.

In this case, any determination of the cloak performance would result in a positive r.m.s. value of the proposed pressure difference. The number of points selected was large enough to capture even the smallest deviation from the ideal cloak performance.

In Eq. (2.43) i is the measurement point index along the wave propagation line (axial direction), which j represents the point index in the lateral directions. Based on this indicator the performance of an anisotropic acoustic cloak surrounding a flexible object is quantified at different excitation frequency values such that the larger the indicator values, the more deterioration in the cloak performance is.

The proposed nonlinear transformations of Akl et al. [35] have proven to improve the way in which the acoustic metamaterial anisotropic cloak works away from the limited frequency values. This is shown in Fig. 2.12 by plotting the performance indicator of the linear cloak and one of the nonlinear cloaking over the

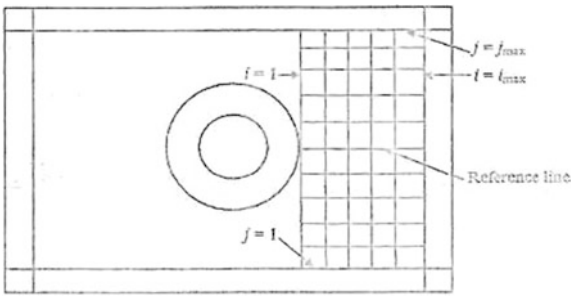

Fig. 2.11 Schematic of the measurement grid points required revaluation the performance indicator. From Akl et al. [35]

frequency range under study. It is clear that the nonlinear cloak performance at frequency ranges away from these domain resonant frequencies is much better. The same conclusion is drawn from Fig. 2.13 where the acoustic pressure field for both the linear and nonlinear transformation for frequency values away from the domain resonance frequency is plotted. In order to show the degree by which the nonlinear transformation has improved the cloaking performance, the difference between the performance indicator values for nonlinear transformation with minimum PI value and those for linear transformation at each frequency is calculated and plotted against the excitation frequency as shown in Fig. 2.14. In this figure, the higher the positive difference, the more improvement of the acoustic cloak performance is achieved. Once more, it is evident that a perfect linear acoustic cloak is achievable only at the same specific frequency values and the proposed nonlinear transformation has improved significantly the way in which the acoustic metamaterial anisotropic cloak works away from the limited frequency values. Although the simulations of the acoustic metamaterial anisotropic cloak around flexible objects encounter some sort of numerical error, the proposed nonlinear transformations open the door for searching for different coordinate transformations function that would lead to simulation results insensitive to the solution domain dimensions.

2.7 Acoustical Cloaking of Underwater Objects

A group at the Mechanical Engineering Department of the University of Illinois led by Nicholas Fang have created a numerical model to build a metamaterial cloak that guides sound waves around objects in water. The model is based on the acoustic lumped circuit network. The unit cell of the network is so small compared to the wavelength of the sound that it becomes and effective anisotropic medium that guides sound flow around the cloaked object. Computer simulations demonstrated that the numerical model successfully achieved a cloaking effect. The next step is to construct and test an actual physical version of the cloak based on that numerical model. If the metamaterial cloak also works, considerably more work needs to be done before the cloak could be scaled up to hide a ship or a submarine. Their mesh

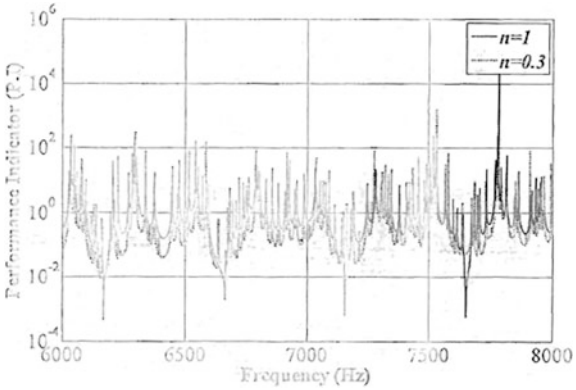

Fig. 2.12 Nonlinear ($n = 0.3$) acoustic cloak performance against the linear cloak when surrounding the host medium at different frequency values. From Akl et al. [35]

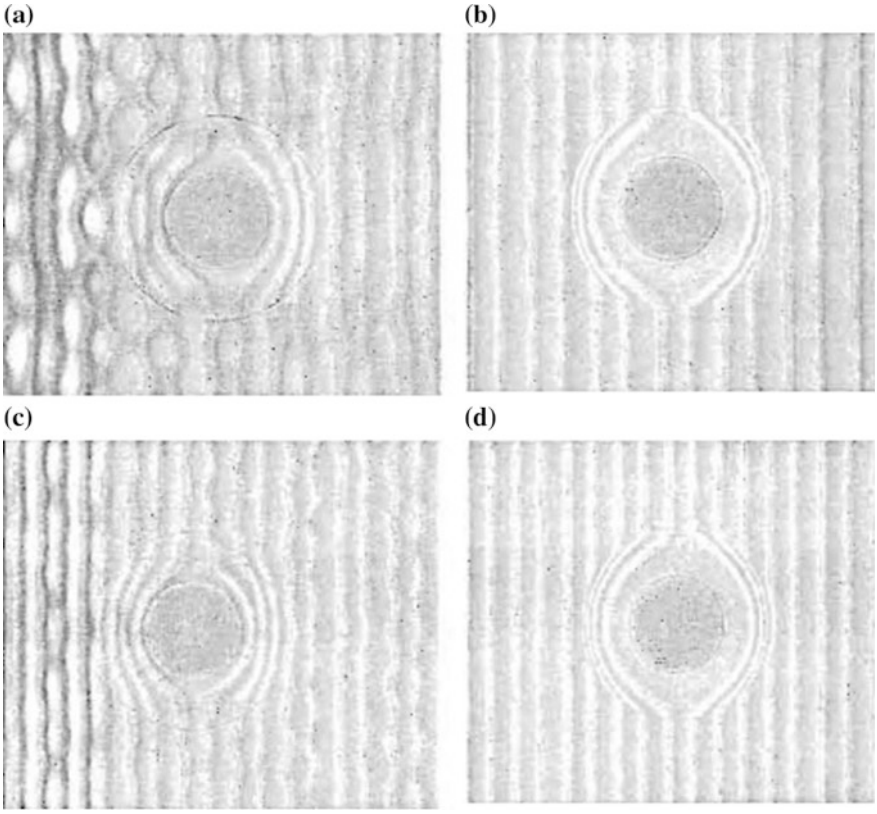

Fig. 2.13 Full wave time-harmonic acoustic pressure field plot of the analyzed ideal cloak with water as base medium: **a** linear at 6000 Hz, **b** nonlinear ($n = 0.3$) at 6000 Hz, **c** linear at 7000 Hz and **d** nonlinear ($n = 0.3$) at 7000 Hz. From Akl et al. [35]

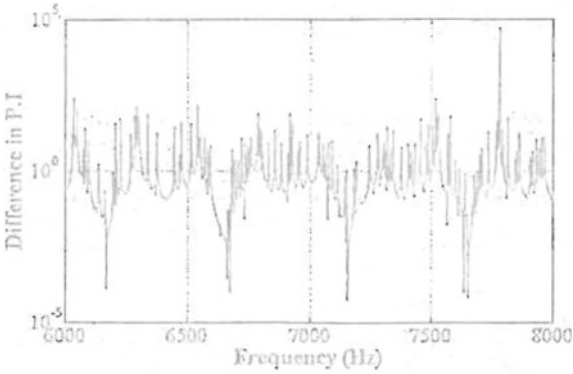

Fig. 2.14 Performance indicator difference between linear and nonlinear cloaks at different frequency values. From Akl et al. [35]

model is based on cloaking an object with a diameter of about 0.67 times the wavelength of light a far cry from the 50-foot beam of a nuclear submarine. Their work is published in the 15 May 2009 issue of the Physical Review Letters [36].

2.8 Extension of Double Negativity to Nonlinear Acoustics

The lossless form of nonlinear acoustic wave equation up to the third-order elastic coefficient can be given by Thurstone and Shapiro [37] as

$$\ddot{u} = \frac{M_2}{\rho_0}\frac{\partial^2 u}{\partial x^2} + \frac{M_3}{\rho_0}\left(\frac{\partial^2 u}{\partial x^2}\right)\left(\frac{\partial u}{\partial x}\right) \tag{2.44}$$

where u = displacement, x = Lagrange coordinate in the direction of motion of a particle and anisotropic solid is used.

Where M_2 is a linear combination of second-order elastic coefficients and M_3 is a linear combination of second- and third-order elastic coefficients.

To allow for energy dissipation, Eq. (2.44) is modified by adding a term to include the frequency dependent attenuation coefficient $\alpha = \alpha(\omega)$, to the right hand side

$$\ddot{u} = \frac{M_2}{\rho}\frac{\partial^2 u}{\partial x^2} + \frac{M_3}{\rho}\left(\frac{\partial^2 u}{\partial x^2}\right)\left(\frac{\partial u}{\partial x}\right) + \frac{2\alpha}{\omega^2}C^3\frac{\partial^2 u}{\partial x^2 \partial t} \tag{2.45}$$

where $C^2 = M_2/\rho$ = speed of propagation of an infinitesimal amplitude sound wave and ρ = mass density of medium.

By replacing ρ by $-\rho$ and M_2 and M_3 by $-M_2$ and $-M_3$. There is no change in the form of equation. Hence, the nonlinear acoustic new equation is also gauged invariant in the mass density and the elastic coefficient.

References

1. Veselago, V.G.: The electrodynamics of substances with simultaneous negative values of ε and μ. Sov. Phys. Usp. **10**(4), 509 (1968)
2. Mandel'stam, L.I.: JETP **15**, 475 (1945)
3. Pendry, J.B., Holden, A.J., Robbins, D.J., Stewart, W.J.: Magnetism from conductors and enhanced non-linear phenomena. IEEE Trans. Microw. Theory Techn. **47**(11), 2075–2984 (1999)
4. Shelby, R.A., Smith, D.R., Schultz, S.: Experimental evidence of a negative index of refraction. Science **292**(5514), 77 (2001)
5. Gan, W.S.: Gauge invariance approach to acoustic fields. In: Akiyama, I. (ed.) Acoustical Imaging, vol. 29, pp. 389–394. Springer, Dordrecht (2007)
6. Cummer, S.A., Schurig, D.: One path to acoustic cloaking. New J. Phys. **9**, 45 (2007)
7. Korringa, J.: Physica (Amsterdam) **XIII**, 392 (1947)
8. Kohn, W., Rostoker, N.: Phys. Rev. **94**, 1111 (1951)
9. Liu, Z., Chan, C.T., Sheng, P., Goertzen, A.L., Page, J.H.: Elastic wave scattering by periodic structures of spherical objects: theory and experiment. Phys. Rev. B **62**(4), 2446–2457 (2000)
10. Sigalas, M.M., Economou, E.N.: J. Sound Vib. **158**, 377 (1992)
11. Kushwaha, M.S., Halevi, P., Dobrzynski, L., Djafrari-Rouhani, B.: Phys. Rev. Lett. **71**, 2022 (1993)
12. Sanchez-Perez, J.V., Caballero, D., Martinez-Sala, R., Rubio, C., Sanchez-Dehesa, J., Meseguer, F.: Phys. Rev. Lett. **80**, 5325 (1998)
13. Kafesaki, M., Economou, E.N.: Phys. Rev. B **52**, 13317 (1995)
14. Yang, S., et al.: Phys. Rev. Lett. **88**, 104301 (2002)
15. Wolfe, J.P.: Imaging Phonons: Acoustic Wave Propagation in Solids. Cambridge University Press, Cambridge, England (1998)
16. Liu, Z., et al.: Phys. Rev. B **62**, 2446 (2000)
17. Zhang, X., Liu, Z.: Negative refraction of acoustic waves in two-dimensional phononic crystals. Appl. Phys. Lett. **85**(2), 341–343 (2004)
18. Luo, C., Johnson, S.G., Joannopoulos, J.D.: Appl. Phys. Lett. **83**, 2352 (2002)
19. Lai, Y., Zhang, X., Zhang, Z.Q.: Appl. Phys. Lett. **79**, 3224 (2001)
20. Pendry, J.B.: Phys. Rev. Lett. **85**, 3966 (2000)
21. Schurig, D., Mock, J.J., Justice, B.J., Cummer, S.A., Pendry, J.B., Starr, A.F., Smith, D.R.: Metamaterial electromagnetic cloak at microwave frequencies. Science **314**, 977–980 (2006)
22. Luo, C., Johnson, S.G., Joannopuolos, J.D., Pendry, J.B.: Phys. Rev. B **65**, 201104 (2002)
23. Pendry, J.B., Schurig, D., Smith, D.R.: Controlling electromagnetic fields. Science **312**, 1780–1782 (2006)
24. Milton, G.W., Briane, M., Willis, J.R.: On cloaking for elasticity and physical equations with a transformation invariant form. New J. Phys. **8**, 248 (2006)
25. Cummer, S.A., Raleigh, M., Schurig, D.: New J. Phys. **10**, 115025–115034 (2008)
26. Cummer, S.A., Rahm, M., Schurig, D.: Material parameters and vector scaling in transformation acoustics. New J. Phys. **10**, 115025 (2008)
27. Cummer, S.A., et al.: Scattering theory derivation of a 3D acoustic cloaking shell. Phys. Rev. Lett. **100**, 024301 (2008)
28. Chen, H., Chan, C.T.: Acoustic cloaking in three dimensions using acoustic metamaterials. Appl. Phys. Lett. **91**, 183518 (2007)
29. Greenleaf, A., Kurylev, Y., Lassas, M., Uhlmann, G.: Comment on "Scattering derivation of a 3D acoustic cloaking shell" (2008)
30. Lee, S.H., Kim, C.K., Park, C.M., Seo, Y.M., Wang, Z.G.: Composite acoustic medium with simultaneously negative density and modulus. In: Proceedings of ICSV17 (2010)
31. Cheng, Y., Xu, J.Y., Liu, X.J.: One-dimensional structured ultrasonic metamaterials with simultaneously negative dynamic density and modulus. Phys. Rev. B **77**, 045134 (2008)

32. Greenleaf, A., et al.: Anistropic conductivities that cannot be detected by EIT. Physiol. Meas. **24**, 413–419 (2003)
33. Yang, S., Page, J.H., Liu, Z., Cowan, M.L., Chan, C.T., Sheng, P.: Focusing of Sound in a 3D Phononic Crystal. Phys. Rev. Lett. **93**(2), 024301-1–024301-4 (2004)
34. Hu, J., Zhou, X., Hu, G.: A numerical method for designing acoustic cloak with arbitrary shapes, Comput. Mater. Sci. **46**, 708–712 (2009)
35. Akl, W. Elnady, T., Elsabbagh, A.: Improving acoustic cloak bandwidth using nonlinear coordinate transformations. In: Proceedings of ICSV17 (2010)
36. Fang, N., Zhang, S.: Phys. Rev. Lett. (2009)
37. Thurston, R.N., Shapiro, M.J.: J. Acoust. Soc. Am. **41**, 1112 (1967)

http://www.springer.com/978-981-10-6375-6

New Acoustics Based on Metamaterials

Gan, W.S.

2018, XVI, 313 p. 69 illus., 25 illus. in color., Hardcover
ISBN: 978-981-10-6375-6